

# DC Link Floating for Grid Connected PV Converters

Attila Balogh, Eszter Varga, and István Varjasi

**Abstract**—Nowadays there are several grid connected converter in the grid system. These grid connected converters are generally the converters of renewable energy sources, industrial four quadrant drives and other converters with DC link. These converters are connected to the grid through a three phase bridge. The standards prescribe the maximal harmonic emission which could be easily limited with high switching frequency. The increased switching losses can be reduced to the half with the utilization of the well-known Flat-top modulation. The suggested control method is the expansion of the Flat-top modulation with which the losses could be also reduced to the half compared to the Flat-top modulation. Comparing to traditional control these requirements can be simultaneously satisfied much better with the DLF (DC Link Floating) method.

**Keywords**—DC link floating, high efficiency, PV converter, control method.

## I. INTRODUCTION

THE improvement of power semiconductors and signal processors led to the new generation of power converters and control strategies. During the last years depending on grid connected converter type, there were some hardware [1]-[4] solutions for increasing the efficiency. The energy, especially the renewable energy, is quite expensive yet. So the efficiency is one of the most critical parameter of a grid connected system. One possible method to increase the efficiency is reducing the switching losses. At grid connected converters the most frequent main circuit arrangement is the three phase bridge [5][6]. In the new converters the developers do everything to reduce the switching losses of the semiconductors. The main circuit is usually unchanged, since the changing cost is quite high. However, with a well designed software solution on the same power circuit arrangement it is possible to reduce the switching losses with

up to 75%. Further critical point is the harmonic emission and power factor correction. In this view there are essential two different types of converters. When the harmonic emission is under the limit but the current waveform is not sinusoidal the converter is called “grid-care”. When the waveform is also sinusoidal it is called grid-friendly converter [7][8]. When a transformer is used for galvanic isolation, we have some freedom for the common mode voltage of the converter. In this case the efficiency can be improved by the flat-top or discontinuous PWM, where the switching losses can be reduced by 50%. Further improvement may be reached – especially at low power – utilizing the 3SC as described in [9]-[14]. Good efficiency at low power has much more importance than one would think for the first look. E.g. in photovoltaic applications the energy generated in one year depends strongly on the efficiency below half of the nominal load, since in most of the time the in-radiation is much below the nominal or peak radiation. Similarly when the load is a drive (e.g. a frequency converter), the converter usually works at its maximal current during acceleration and deceleration, while in most of the time the load is much below the nominal current. In both cases the average efficiency depends strongly on the efficiency at low power.

## II. THE STRUCTURE OF THE CONVERTER

The main parts of the converter are: the PV array, the Boost DC/DC converter and the three phase inverter with filters (see Fig. 1). The PV array converts the solar energy to DC power. The step-up converter may raise the voltage level of the PV array to the voltage level of the three phase bridge.

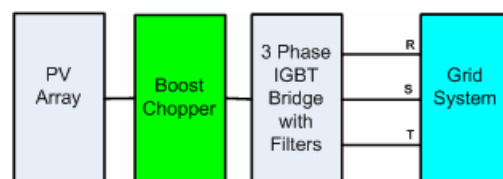


Fig. 1 Topology of the converter

The control of the boost chopper algorithm includes the maximal power point tracking (MPPT). The three-phase bridge converts the dc voltage to nearly sinusoidal ac currents. The high order harmonics of the output current are filtered out by passive low-pass filter. The main circuit arrangement can be seen in Fig.2. The diode of the  $4H$  IGBT,  $4L$  IGBT,  $L_b$

Manuscript received April 28, 2008

Attila Balogh is with the Budapest University of Technology and Economics, Department of Automation and Applied Informatics, Budapest, Hungary (phone: +36 (1) 463 1552, fax: +36 (1) 463 2871, e-mail: balogh@aut.bme.hu).

Eszter Varga is with the Budapest University of Technology and Economics, Department of Automation and Applied Informatics, Budapest, Hungary (phone: +36 (1) 463 1552, fax: +36 (1) 463 2871, e-mail: hukk01@gmail.com).

Istvan Varjasi, PhD, is with the Budapest University of Technology and Economics, Department of Automation and Applied Informatics, Budapest, Hungary (phone: +36 (1) 463 1552, fax: +36 (1) 463 2871, e-mail: varjasi@aut.bme.hu).

inductor and  $C_b$  capacitor are the boost converter and  $C_{pv}$  is the filter capacitor of the PV array. In the followings it is assumed that  $C_{pv}$  is much greater than  $C_b$ .

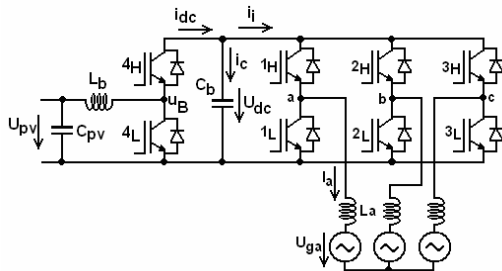


Fig. 2 The main circuit

### III. THE TRADITIONAL CONTROL

There are several control methods of the grid connected PV converter. Most of them consist of an outer control loop for the DC voltage and inner current control loop. From these we use the grid voltage oriented current control. This control structure is very similar to the field oriented control (FOC) of ac machines. The controllers work here also in a rotating frame, but this rotating frame is connected to the grid voltage vector, so we may name this control system as grid voltage oriented control. The current component in the direction of the grid voltage vector is named as current "d" and is proportional to active power, while the orthogonal current component is named as current "q" and is proportional to reactive power. In this arrangement there is no zero order current, so it is enough to measure only two currents. The phase currents are transformed to the rotating d-q coordinate-system [2]. For the current control the currents are sampled at symmetry point(s) of PWM cycle, so the sampled current is close to the average value for a given switching period.

### IV. THE SUGGESTED CONTROL METHOD

The developed inverter control has to satisfy two groups of requirements. On one hand the dc source energy should be feed-back to the ac network with an efficiency as high as possible. On the other hand the prescriptions of the standards must be full-filled for the utility compatibility. According to the standards, the ac currents should be nearly sinusoidal, and the power factor should be greater than 0.95. By reduction of the switching losses with the proposed method we may increase the efficiency while maintaining the limitations of standards. In case of PV converters the efficiency can be calculated as the weighted average of efficiencies measured at the 10%, 50% and 90% of nominal power [7]. Our method is based on the Flat-top modulation therefore in the followings a brief summary is given about it.

The main aim of this modulation type is to decrease the switching losses of the inverter. The switching losses are nearly proportional to the switched voltage, the switched current and the switching frequency. The switched voltage is

defined by the DC voltage, which should be controlled to the possible minimal value to minimize the switching losses. We still have the multiplicand of the switched current and switching frequency. With other words we should avoid switching in a phase as much as possible, when the current in that phase is large. For the grid-connected inverters the power-factor is close to one (should be above 0.95), so the curve of the phase voltage is nearly proportional to the curve of the current. As a result we avoid switching in the phase which has the highest voltage absolute value in the next switching period. The shape depends on the modulation depth.

At the limit of modulation depth for the sinusoidal output the duty cycle is  $1/\sqrt{3}$  (see Fig. 3.a).

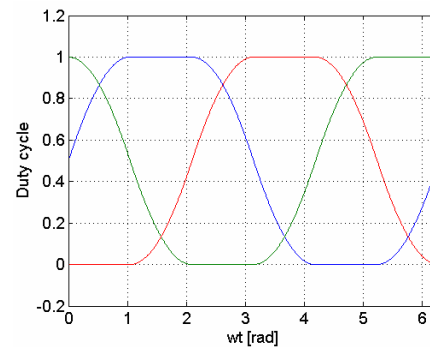


Fig. 3.a Flat-top PWM, 100% modulation depth

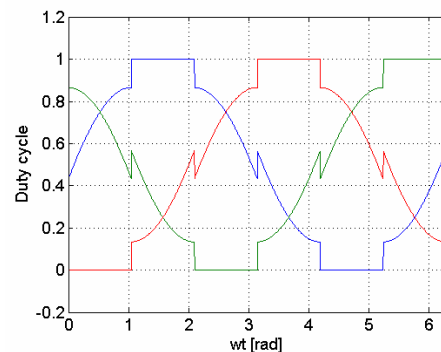


Fig. 3.b Flat-top PWM, 90% modulation depth

Under the sinusoidal limit the shapes look according to Fig. 3.b.

With the Flat-top modulation the switching losses could be reduced by nearly 50%. A drawback arises with small modulation depth, since in that case the spectra of the common-mode voltage is pretty wide, which could result in complicated and expensive EMI filters.

In the followings the description of the DLF is presented.

#### A. The Base Idea

The DLF method tries to reduce the switching losses with the floating of the DC link voltage. The available voltage vectors of a voltage source inverter can be seen in Fig.4. In the first step it is assumed that the current controller works

between the point A and B and Flat-top modulation is used. In this case the switching losses are small, since in this section only the IGBTs of the third leg are switched from (1,0,0) to (1,0,1).

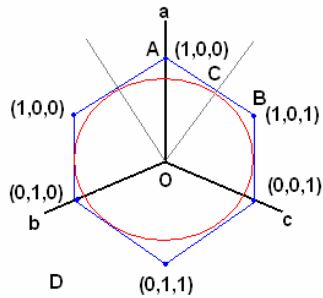


Fig. 4 Voltage vectors

Due the Flat-top modulation the IGBTs are not switched in the area, where the current is the maximal causing smaller switching losses. In point C the available voltage (see blue curve in Fig.3.), which depends on the DC link voltage, is equal to the inverter output voltage (see red curve in Fig.4.). If we could modulate the DC link voltage in order to it approaches the inverter output voltage in a big amount of the switching period, the switching losses will be much smaller than with the standard control methods. The DLF method uses such the aforementioned floating.

#### B. The Modulation Method

In this subsection the modulation method and the switching losses are investigated. In point A the difference between the available and inverter output voltage is 14% of the DC link voltage. If we modulate the DC link voltage in this point, the 14% voltage change would be able to remove the PV array from its maximal power point (MPP). We estimated that 6% voltage change is small enough to keep the PV array in MPP. With 6% DC link modulation the non switching area will be longer with  $\alpha_1$ . This angle can be calculated as follow:

$$\alpha_1 = \arccos(1 - 0.06) \approx 20^\circ \quad (1)$$

In the next step the switching losses are calculated in case of sinusoidal, Flat-top and Flat-top-DLF hybrid modulation. We assume that the switching losses are proportional to the switched current at constant switching frequency.

The switching losses ( $P_d$ ) of the sinusoidal modulation can be calculated as follow:

$$P_d = \int_0^{\pi/2} \sin(\omega t) d\omega t = [-\cos(\omega t)]_0^{\pi/2} = 1 \quad (2)$$

In (2) it is assumed that the IGBTs are switched in the whole of the half period.

In case of Flat-top modulation the IGBTs are not switched in that  $60^\circ$  of the switching period where the phase current is the maximal. In this case the switching losses are:

$$P_d = \int_0^{\pi/3} \sin(\omega t) d\omega t = [-\cos(\omega t)]_0^{\pi/3} = 0.5 \quad (3)$$

From (3) it is seen that with Flat-top the half of the switching losses can be saved.

With the Flat-top-DLF hybrid modulation above the aforementioned  $60^\circ$  area in further  $20^\circ$  are not switched the IGBTs, so the switching losses can be calculated as follow:

$$P_d = \int_0^{2\pi/9} \sin(\omega t) d\omega t = [-\cos(\omega t)]_0^{2\pi/9} = 0.23 \quad (3)$$

With this modulation technique compared to the Flat-top modulation about further 50% switching losses decrease can be reached.

#### C. The Converter Control

There are two possible methods to control the converter.

In the first case the booster tries to keep the PV array in the maximal power point and the inverter floats the DC link voltage. When the switching frequency of the booster is high enough, than the current of the  $L_b$  inductor will be nearly constant. In this case the value of the DC link current depends only on the DC link voltage. If the inverter floats the DC link voltage with about 6% of nominal voltage than due the six-side symmetry there will be an about 6% of nominal current  $6^{\text{th}}$  order harmonic current in the DC link. This harmonic current will cause  $5^{\text{th}}$  and  $7^{\text{th}}$  order current harmonics on the AC side. In case of PV converters the standard prescribes that the maximal total harmonic distortion (THD) of the grid current has to be less than 5% of the nominal current. If the converter floats the DC link voltage the current THD is unsupportable.

In the second case the booster floats the DC link voltage. The floating only in that case works when the capacitor of the PV array ( $C_{pv}$ ) is much greater than the booster capacitor ( $C_b$ ). In this case changes the standard control strategy in which the booster controls the MPP and the inverter tries to control nearly constant DC voltage. In case of Flat-top-DLF hybrid modulation the booster prescribes the phase current references for the inverter legs in which the current is maximal, while the current control of the third leg is made by the inverter. We observe that in the third phase in this area the current reference otherwise is almost zero.

The DLF affect on the MPP, however, we assume that with the 6% floating on the DC link the loss due the floating in the MPP is less than the saved switching losses on the inverter side.

#### D. Possible Modulation Techniques

There are three modulation modes which can be used in this case.

- Standard Flat-top modulation, in this case the half of the switching losses can be saved.

- Flat-top-DLF hybrid modulation (in the third leg there is not special modulation). In this case further 25% of the switching losses can be saved.
- Flat-top-DLF-3SC hybrid modulation. In this case the aforementioned hybrid modulation is completed with 3SC modulation in the 3rd leg. The 3SC (three state current control) is a special efficiency increase method which tries to decrease the switching losses with the utilization of the discontinuous current mode [9]-[14].

The DC link floating can be also used in the maximal power point tracking methods, however, due the relatively high floating frequency (about 300Hz) the MPP sensors have to be compensated.

### V. THE MATHEMATICAL MODEL

In this section the mathematical description of DLF modulation technique is presented.

The available voltage vectors and the control sections of the DLF method can be seen in Fig. 5. In Fig. 5 the red curve is the base harmonic voltage vector ( $U_1$ ) and the blue curve is the available DC voltage. In case of DLF control the first section (from point A to point B) is divided into further three subsections.

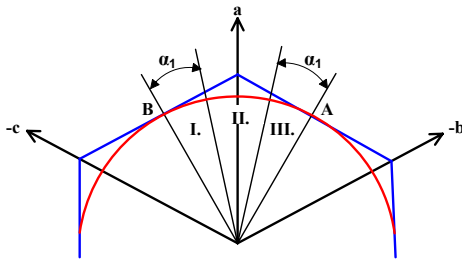


Fig. 5 Voltage vectors in DLF

Subsection I and III represent the DLF non switching area (see IV.B) while in subsection II the standard Flat-top modulation is used.

In the followings the applicable modulation technique is investigated in each control sections. In first step let's assume that the DC link voltage ( $U_{dc}$ ) is constant. In this case the maximal base harmonic voltage amplitude is the following:

$$|\bar{U}_{\max}| = \frac{U_{dc}}{\sqrt{3}} \frac{1}{\cos \rho} \quad (4)$$

where  $\rho$  is the actual angle of the grid voltage. When the base harmonic voltage is constant than the DC voltage can be calculated as follow:

$$U_{dc} = \sqrt{3} U_1 \cos \rho \quad (5)$$

In the next step let's investigate that what kind of modulation signal would be the best in each of the subsections.

The determined modulation signals can be seen in Fig. 6.

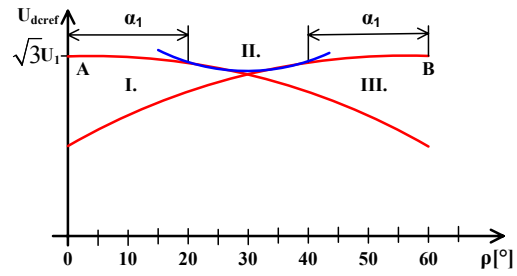


Fig. 6 DC voltage in the subsections

In subsection I the DC voltage reference ( $U_{dcref}$ ) should be the followings:

$$U_{dcref} = \sqrt{3} U_1 \cos \rho \quad (6)$$

In subsection III the voltage reference is similar to the voltage reference in subsection I and can be calculated as follow:

$$U_{dcref} = \sqrt{3} U_1 \cos(\rho - 60^\circ) \quad (7)$$

In section II a DC voltage reference curve has to be fitted to (6) and (7). The parametric form of to be fitted reference curve is the following:

$$U_{dcref} = A - B \cos(\rho - 30^\circ) \quad (8)$$

The parameters can be determined from the following conditions:

- The voltage reference curve in  $\alpha_1$  has to be equal to (6) and (7) in  $\alpha_1$ .
- The change of rate of the voltage reference curve in  $\alpha_1$  has to be equal to the rate of change of (6) and (7) in  $\alpha_1$ .

From the aforementioned conditions and from (8) the parameters are the follows:

$$A = \sqrt{3} U_1 \left( \cos \alpha_1 - \frac{\cos(\alpha_1 - 30^\circ) \sin \alpha_1}{\sin(\alpha_1 - 30^\circ)} \right)$$

$$B = - \frac{\sqrt{3} U_1 \sin \alpha_1}{\sin(\alpha_1 - 30^\circ)} \quad (9)$$

The time function of the DC voltage reference is already known. The DC voltage is controlled by booster, so in next step the control of the booster should be investigated.

The booster capacitor current (see Fig. 2) from (6)-(8) can be calculated as follow:

$$i_c(t) = C_B \frac{dU_{dcref}(t)}{dt} \quad (10)$$

Assuming constant power generation the inverter current is the following:

$$i_i(t) = \frac{P}{U_{dcref}(t)} \quad (11)$$

where  $P$  is the power transferred into the grid.

The booster current ( $i_{dc}$ ) is the sum of (10) and (11):

$$i_{dc}(t) = \frac{P}{U_{dcref}(t)} + C_B \frac{dU_{dcref}(t)}{dt} \quad (12)$$

The potential ( $u_B$ ) of 4H and 4L IGBTs (see Fig. 2) is the following:

$$u_B = d * U_{dcref}(t) \quad (13)$$

where  $d$  is the duty cycle of IGBT 4H. Assuming lossless booster the input side and output side power have to be equal, so the current of the booster inductance ( $L_b$ ) can be calculated as follow:

$$i_B = \frac{1}{d} i_{dc}(t) \quad (14)$$

The voltage of the booster inductance can be calculated as follow:

$$U_{PV} - U_B = i_B R + L \frac{di_B}{dt} \quad (15)$$

From (13)(14) and (15) the rate of change of the booster inductance's can be calculated as follow:

$$\frac{di_B}{dt} = \frac{1}{L_b} \left( U_{PV} - \frac{i_{dc} * U_{dcref}}{i_B} - i_B R \right) \quad (16)$$

Finally the duty cycle of the booster is the following:

$$d = \frac{i_B}{i_{dc}} \quad (17)$$

The efficiency of the DLF control was verified with some simulations. The results are presented in the next section.

## VI. EXPERIMENTAL RESULTS

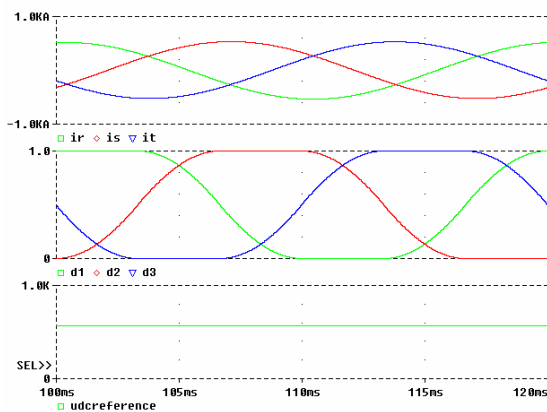


Fig. 7 Simulation results (Flat-top)

In this section simulation results are given to verify the effectiveness of the Flat-top-DLF control method. In Fig. 7

the duty cycles, the grid currents and the DC link voltage of Flat-top modulation while in Fig. 8 the aforementioned curves of DLF modulation can be seen.

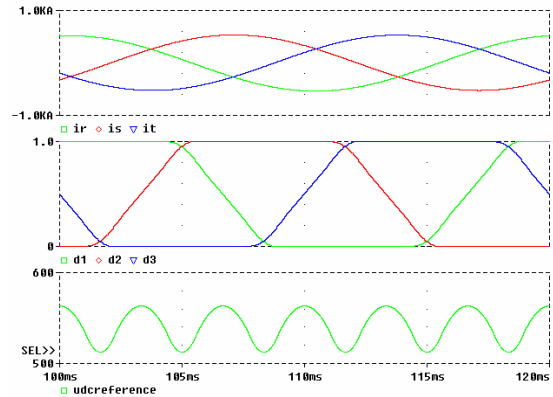


Fig. 8 Simulation results (DLF)

In the upper diagram (see Fig. 7) the sinusoidal grid currents, in the middle one the duty cycles' of the Flat-top modulation while in the third one the DC link voltage can be seen. It is seen that in case of Flat-top modulation the DC link voltage is constant and the IGBTs are not switched in that 60° period when the voltage and the current is almost maximal.

In the upper diagram (see Fig. 8) the sinusoidal grid currents, in the middle one the duty cycles' of the DLF modulation while in the third one the DC link voltage can be seen. It is seen that in case of DLF modulation the DC link voltage changes according to the DC voltage reference which was calculated in section V. The IGBT's non switching area is extended to about 100° of the switching period when the voltage and the current is almost maximal, so the switching losses were reduced with 25% compared to the Flat-top modulation.

## VII. CONCLUSION

With the new developed DC link floating control we could make a high efficiency and reliable PV converter, which satisfy the prescriptions and limitations of the standards. The DLF control was verified with some simulation, and it is work correctly in the whole load range. Our future plan is to complete and verify the DFL method with the auxiliary DLF-3SC control with which we could further increase the efficiency.

## REFERENCES

- [1] P. Wood, *Switching Power Converters*. Van Nostrand Reinhold Company, New York, 1981.
- [2] H. W. van der Broeck, H. Ch. Skudelny, and G. Stanke, Analysis and realization of a pulse width modulator based on voltage source space vectors. *IEEE Transactions on Industrial Applications*, vol 24, pp 142-150, 1988.
- [3] S. Ogasawara, H. Agaki, and A. Nabae, A novel PWM scheme of voltage source inverter based on space vector theory. *Conference record European Power Electronics Conf.*, pp 1197-1202, 1989.

- [4] G. Buja and G Indri, Improvement of pulse width modulation techniques, *Arch Elektrotech. (Germany)*, vol 57, pp 281-289, 1975.
- [5] T. Shimizu, M.Hirakata, T. Kamezawa, H. Watanabe, Generation Control Circuit for Photovoltaic Modules. *IEEE Trans. On Power Electronics*, Vol. 16, No. 3, May, 2001, pp. 293
- [6] R.W. Erickson, D. Maksimovic, Fundamentals of Power Electronics. *Kluwer Academic Pub; March 1, 1997, ISBN: 0-412-08541-0, 773 pages.*
- [7] UL 1741, UL Standard for inverters, converters, and controllers for use in independent power production systems, *Northbrook, 2001*
- [8] IEC 61727 International Standard, Photovoltaic (PV) systems – Characteristics of the utility interface, *Switzerland, 2004.*
- [9] A. Balogh, I. Varjasi, Discontinuous Current Mode of a Grid Connected PV Converter, *IYCE2007, Budapest, Hungary*
- [10] I. Varjasi, A. Balogh, S. Halasz, Sensorless control of a grid connected PV converter, *EPE-PEMC2006, Portoroz., Slovenia.*
- [11] A. Balogh, Z.T. Bilau and I. Varjasi, High Efficiency Control of a Grid Connected PV Converter. *In Proc. of EuroPES2007, Palma de Mallorca, Spain.*
- [12] Attila Balogh, Zoltán Tamás Bilau, Istvan Varjasi Control Algorithm for High Efficiency Grid Connected PV Converters. *In Proc. of IWCIT 2007, Ostrava, Czech Republic*
- [13] Attila Balogh, Eszter Varga, István Varjasi: 3SC for Grid Connected Converters, *In Proc. of Power and Energy Systems Conference (EuroPES 2008), Corfu, Greece, 2008.*
- [14] Attila Balogh, Zoltan Tamás Bilau, István Varjasi, Sándor Halász: High Efficiency Control of a Low Noise PV Converter, *In Proc. of Mezsduarodnaja Naucsno-Tehnicoszskaja Konferencija, Tomszk, Russia, 2007.*



**Attila Balogh** was born on March 5 1982 in Pápa, received the Electrical Engineering degree from the Budapest University of Technology and Economics, Budapest, Hungary, in 2006. Since 2006, he has been a Ph.D. student in the Department of Automation and Applied Informatics at the Budapest University of Technology and Economics (BUT). His research field involves control strategies, FPGA based process control,

servo drives and renewable energy.

He has attended international conferences several times and has worked in some research projects, as well.

Mr. Balogh is member of Hungarian Electrotechnical Association.



**Eszter Varga** was born on November 21 1983 in Szekszárd, she is an Architect student at the Budapest University of Technology and Economics (BUT). Her research field involves application of renewable energy sources, buildings-constructions for solar technology and efficiency increasing methods for PV cells.

She has attended international conferences several times and has worked in some research projects, as well.

Ms. Varga is member of ESN.



**István Varjasi** was born on September 20 1956 in Soltvadkert, received the Electrical Engineering and Ph.D. degrees from the Budapest University of Technology and Economics, Budapest, Hungary, in 1980 and 1997. Since 1998, he has been an Associate Professor in the Department of Automation and Applied Informatics at the Budapest University of Technology and Economics (BUT). His research field involves

control strategies, FPGA based process control, servo drives and renewable energy.

He has attended international conferences several times and has worked in some research projects, as well.

Dr. Varjasi is member of Hungarian Electrotechnical Association.